Magnetic and Electrical Properties of the Intermetallic Compounds RE_2Au_2Sn (RE = Y, Dy – Tm, Lu) and RE_2Au_2In (RE = Ho, Lu)

Rainer Pöttgen[a], Reinhard K. Kremer[b], Sudhindra Rayaprol[a], Birgit Heying[a], and Rolf-Dieter Hoffmann[a]

[a] Institut für Anorganische und Analytische Chemie, Universität Münster, Corrensstraße 30, D-48149 Münster, Germany
[b] Max-Planck-Institut für Festkörperforschung, Heisenbergstraße 1, D-70569 Stuttgart, Germany

Reprint requests to Prof. Dr. R. Pöttgen. E-mail: pottgen@uni-muenster.de

Z. Naturforsch. **2007**, *62b,* 169 – 172; received October 12, 2006

The intermetallic compounds RE_2Au_2Sn (RE = Y, Dy–Tm, Lu) and RE_2Au_2In (RE = Ho, Lu) were synthesized from the elements *via* arc-melting and subsequent annealing at 1070 K for 10 days. Depending on the size of the rare earth element, the compounds crystallize with the Mo_2B_2Fe-type (space group $P4/mbm$) or the Er_2Au_2Sn structure (space group $P4_2/mnm$), a superstructure of Mo_2B_2Fe. Temperature dependent susceptibility measurements of Y_2Au_2Sn, Lu_2Au_2Sn, and Lu_2Au_2In indicate Pauli paramagnetism compatible with the metallic behavior deduced from resistivity measurements. Ho_2Au_2In and RE_2Au_2Sn (RE = Dy–Tm) show Curie-Weiss behavior above 50 K with experimental magnetic moments close to the free ion values of the trivalent rare earth elements. The compounds Ho_2Au_2In, Dy_2Au_2Sn, Ho_2Au_2Sn, and Er_2Au_2Sn, undergo magnetic ordering at 20(1) (F), 16(1) (AF), 8(1) (AF), and 4.5(1) K (AF), respectively. Tm_2Au_2Sn remains paramagnetic down to 2 K.

Key words: Solid State Synthesis, Magnetism, Electrical Resistivity

Introduction

The rare earth metal (RE) or actinoid (An) based intermetallic compounds RE_2T_2X and An_2T_2X (T = late transition metal; X = In, Sn) with tetragonal Mo_2B_2Fe [1] or Er_2Au_2Sn (U_2Pt_2Sn) structure [2, 3] have intensively been investigated in recent years. Especially the cerium based rare earth compounds have been studied exhaustively. A detailed summary is given in a recent review [4].

So far, with the rare earth elements, only the series of RE_2Pd_2In [5 – 7] and RE_2Cu_2In [8 – 10] indides have been systematically studied with respect to their magnetic and electrical behaviour. Some preliminary magnetic data have been reported for the RE_2Rh_2In [11] and RE_2Pt_2In [12] series by Hulliger.

The structural chemistry of the RE_2Au_2In indides [13, 14] and the RE_2Au_2Sn [2, 13] stannides has been published. The crystal structures of these intermetallic compounds depend on the size of the rare earth elements. With the larger RE atoms (Gd and Tb for RE_2Au_2Sn; Y, Gd–Er for RE_2Au_2In) they adopt the Mo_2FeB_2-type, while the Er_2Au_2Sn (U_2Pt_2Sn)-type superstructure occurs for the compounds with the smaller rare earth elements. We have now systematically investigated the properties of these intermetallics. The magnetic and electrical properties of those RE_2Au_2Sn and RE_2Au_2In compounds which have been obtained in pure form are reported in the following.

Experimental Section

Starting materials for the preparation of the RE_2Au_2Sn stannides and RE_2Au_2In indides were ingots of the rare earth elements (Johnson-Matthey), gold wire (Degussa, ∅ 1 mm), a tin bar (Heraeus), and indium tear drops (Johnson-Matthey), all with stated purities better than 99.9 %. In a first step the rare earth metal pieces were arc-melted [15] to small buttons under an atmosphere of *ca.* 600 mbar argon. The argon was purified over molecular sieves, silica gel, and titanium sponge (900 K). This pre-melting procedure reduces shattering of the sublimed rare earth pieces during reaction with the other elements. The arc-melted rare earth buttons were then mixed with pieces of the gold wire and pieces of indium (tin) in the ideal 2 : 2 : 1 atomic ratio. These mixtures were then arc-melted to buttons. Each product was remelted three times to ensure homogeneity. The weight losses after the various melting procedures were always smaller than 0.5 weight%. The product buttons were

then sealed in pre-heated, evacuated silica tubes and annealed for 10 days at 1070 K. The RE_2Au_2Sn stannides and RE_2Au_2In indides are silvery in compact polycrystalline form; powders are dark grey. All samples are stable in moist air for years.

The samples were characterized *via* X-ray powder diffraction using the Guinier-Simon technique [16] with Cu$K_{\alpha1}$ radiation and silicon (a = 543.07 pm) as an internal standard. The experimental patterns were compared with calculated ones [17], using the positional parameters of Dy_2Au_2In [13] and Er_2Au_2Sn [2] and the lattice parameters of the respective compounds. All samples used for the susceptibility measurements showed only the reflections of the RE_2Au_2In and RE_2Au_2Sn compounds and were thus single-phase materials on the detection level of X-ray powder diffraction.

Susceptibility measurements were performed on a MPMS SQUID magnetometer (Quantum Design) or PPMS (Quantum Design) in the temperature range 2 – 300 K at magnetic field strengths up to 5.5 T (MPMS) and 9 T (PPMS). Gelatine capsules were used as container material. The samples were generally cooled to the lowest temperature in zero magnetic field and then heated in the applied magnetic field. The electrical resistivities were determined with a standard four-probe technique. Thin gold wires and a conducting silver paste were used to apply electrical contacts. The polycrystalline samples of Y_2Au_2Sn, Dy_2Au_2Sn, and Lu_2Au_2Sn were cut into well shaped blocks with a diamond saw. For the other measurements we used irregularly shaped pieces.

Results and Discussion

Magnetic properties

The temperature dependence of the magnetic susceptibility of Y_2Au_2Sn and Lu_2Au_2X (X = In, Sn) is displayed in Fig. 1. Above 100 K the susceptibility is almost independent of the temperature with r. t. values of $5(1) \times 10^{-5}$ emu mol^{-1} (Y_2Au_2Sn), $2.9(1) \times 10^{-5}$ emu mol^{-1} (Lu_2Au_2Sn), and $9.5(2) \times 10^{-4}$ emu mol^{-1} (Lu_2Au_2In). The small susceptibility values are indicative of Pauli paramagnetism of the conduction electrons, as expected for these metallic materials. The increase of the susceptibility towards low temperature is due to traces of paramagnetic impurities.

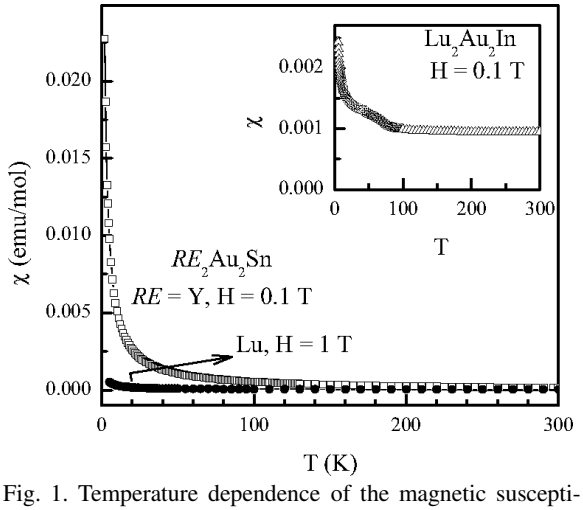

Fig. 1. Temperature dependence of the magnetic susceptibility of Y_2Au_2Sn (0.1 T data), Lu_2Au_2Sn (1 T data), and Lu_2Au_2In (0.1 T data).

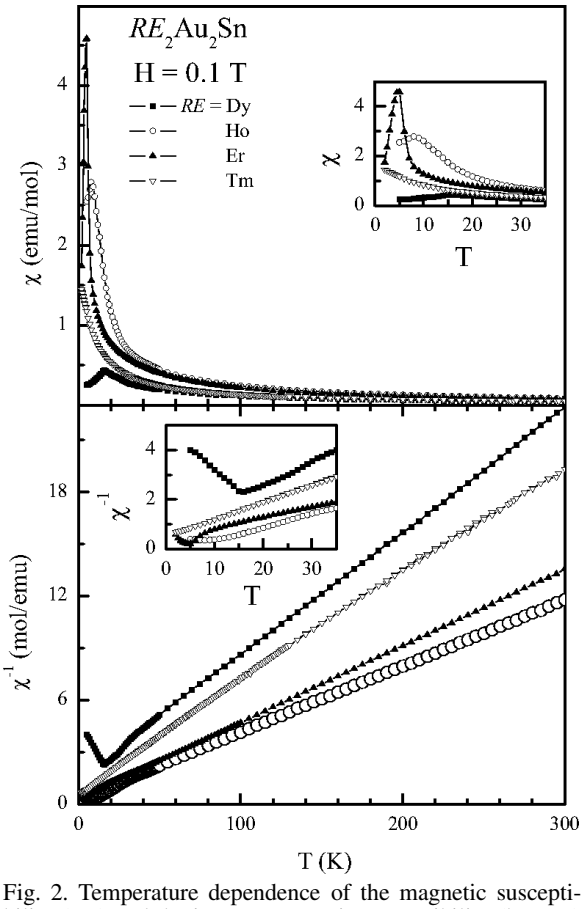

Fig. 2. Temperature dependence of the magnetic susceptibility (top) and the inverse magnetic susceptibility (bottom) of Dy_2Au_2Sn, Ho_2Au_2Sn, Er_2Au_2Sn, and Tm_2Au_2Sn measured at a magnetic flux density of 0.1 T.

All other RE_2Au_2Sn and RE_2Au_2In compounds show Curie-Weiss paramagnetism above 50 K (Fig. 2). The values of the paramagnetic Curie temperatures (Θ) and the effective magnetic moments (μ_{eff}) have been derived from the linear regions (typically above 50 K) from χ^{-1} *vs.* T plots, and are summarized in Table 1. The negative Weiss constants are indicative of predom-

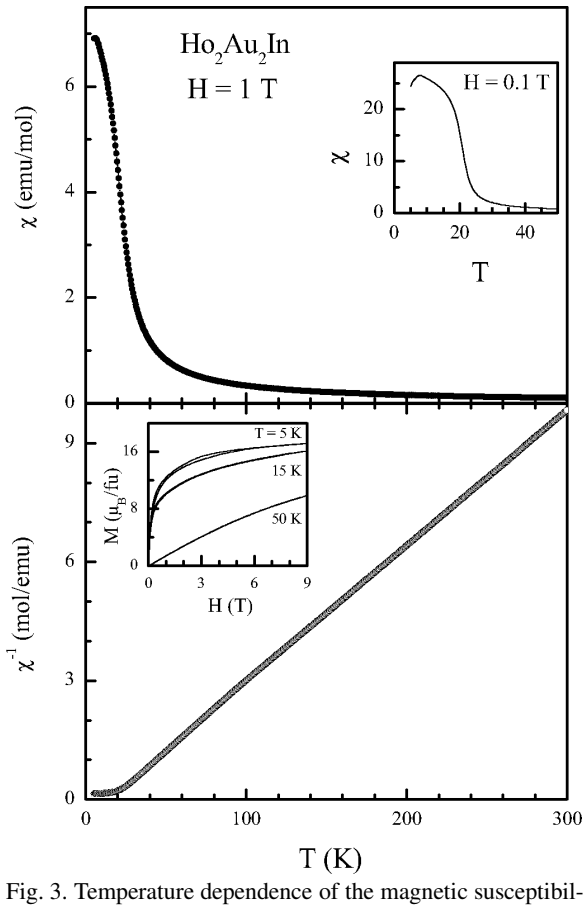

Fig. 3. Temperature dependence of the magnetic susceptibility and the inverse magnetic susceptibility of Ho_2Au_2In measured at a magnetic flux density of 1 T. The inset in the top panel shows on an expanded scale the low temperature features of $\chi(T)$ measured in H = 0.1 T. In the second inset in the bottom panel, low temperature magnetization behaviour (M *vs.* H) is shown.

inant antiferromagnetic interactions. For Dy_2Au_2Sn, Ho_2Au_2Sn, and Er_2Au_2Sn the observed Néel temperatures are 16(1), 8(1), and 4.5(1) K, respectively. As expected from the de Gennes rule, the Néel temperature decreases from the dysprosium to the erbium stannide. Tm_2Au_2Sn shows no magnetic ordering down to 2 K (Fig. 2), although the paramagnetic Curie temperature is also negative.

Ho_2Au_2In has complex magnetic behaviour (Fig. 3). Above 50 K, it behaves as a paramagnet, and the corresponding data from fitting in this region are listed in Table 1. The positive value of the Curie temperature indicates predominant ferromagnetic exchange. Indeed, Ho_2Au_2In is ordered ferromagnetically at 20(1) K (determined from the inflection point of the χ *vs.* T curve)

Table 1. Magnetic properties of the stannides RE_2Au_2Sn (RE = Y, Dy-Tm, Lu) and the indides RE_2Au_2In (RE = Ho, Lu)[a].

Compound	Structure type	Magnetic behavior[a]	μ_{exp} (μ_B)	$\mu_{eff}(Ln^{3+})$ (μ_B)	Θ (K)	$T_{C/N}$ (K)
Stannides:						
Y_2Au_2Sn	Er_2Au_2Sn	PP	–	–	–	–
Dy_2Au_2Sn	Er_2Au_2Sn	AF	10.6(1)	10.65	−20(1)	16(1)
Ho_2Au_2Sn	Er_2Au_2Sn	AF	10.3(1)	10.61	−10(1)	8(1)
Er_2Au_2Sn	Er_2Au_2Sn	AF	9.5(1)	9.58	−7(1)	4.5(1)
Tm_2Au_2Sn	Er_2Au_2Sn	P	8.1(1)	7.56	−21(1)	–
Lu_2Au_2Sn	Er_2Au_2Sn	PP	–	–	–	–
Indides:						
Ho_2Au_2In	Mo_2B_2Fe	F/AF	10.8(1)	10.61	12(1)	20(1)[b]
Lu_2Au_2In	Er_2Au_2Sn	PP	–	–	–	–

[a] The experimentally determined magnetic moments μ_{exp} obtained from the Curie-Weiss law according to $\mu_{exp} = 2.83[\chi\ (T - \Theta)]^{1/2}\ \mu_B$ are compared with the theoretical moments μ_{eff} calculated from the relation $\mu_{eff} = g\ [J\ (J + 1)]^{1/2}\ \mu_B$. The paramagnetic Curie temperatures Θ and the magnetic ordering temperatures T_C and T_N are also listed. PP: Pauli paramagnetism; P: paramagnetism; AF: antiferromagnetism; F: ferromagnetism. [b] Ho_2Au_2In exhibits an additional magnetic transition (spin reorientation) at 7.0(5) K.

and undergoes a spin reorientation at the second magnetic transition temperature of 7.0(5) K. Similar behaviour has been observed by Hulliger [14], however, traces of impurity phases were seen in this sample. In the inset in top panel of Fig. 3, we show $\chi(T)$ measured in a field of 0.1 T, for Ho_2Au_2In on an expanded scale, to illustrate the features at low temperatures. Both magnetic transitions can be clearly seen here.

In the second inset in Fig. 3, we show the magnetization (M *vs.* H) behaviour of Ho_2Au_2In measured at T = 5, 15 and 50 K. At 5 K, in the magnetically ordered state, M increases rapidly for small changes in field (H), but does not saturate as expected for a ferromagnetic compound. However at 90 kOe the maximum magnetization reached (saturation magnetization) is about 8 μ_B/Ho atom, which is about 2 μ_B less than the value expected for Ho^{3+}. This discrepancy can be attributed to crystal field effects and / or magnetic anisotropy in this compound.

Electrical properties

The temperature dependence of the reduced electrical resistivities of RE_2Au_2Sn (RE = Y, Dy, Lu) and RE_2Au_2In (RE = Ho, Lu) is presented in Figs. 4 and 5. Because the samples contained several micro cracks and were irregularly shaped, only the reduced resistivities (R/R_{290}) are plotted here. The R/R_{290} decreases with decreasing temperature for all five compounds, exhibiting metallic behaviour. This is consistent with

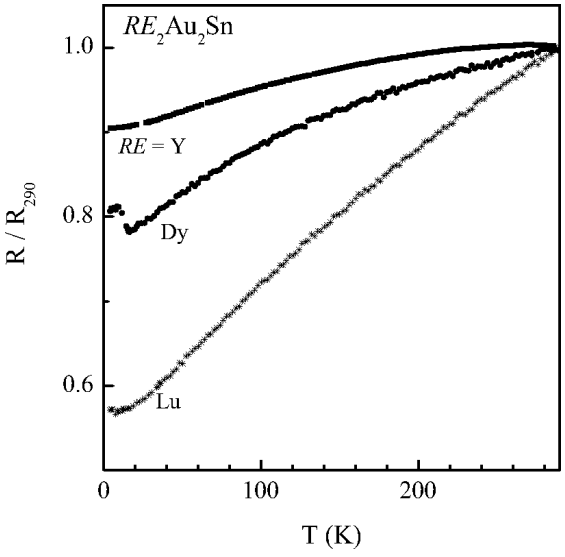

Fig. 4. Temperature dependence of the reduced electrical resistivity $R(T)/R(290\ \mathrm{K})$ of Y_2Au_2Sn, Dy_2Au_2Sn, and Lu_2Au_2Sn.

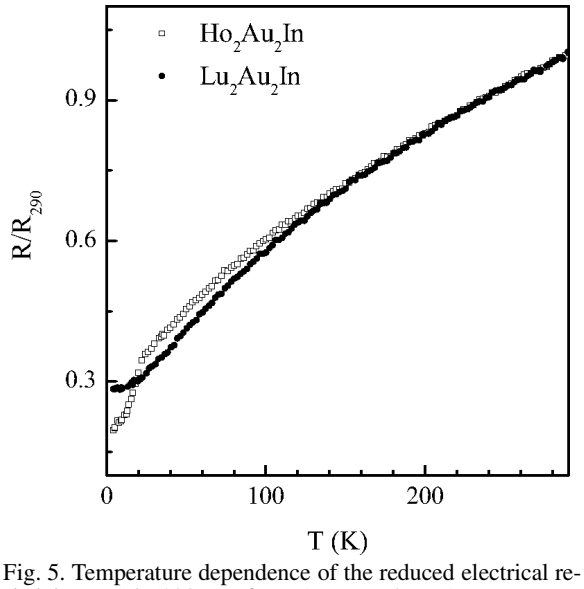

Fig. 5. Temperature dependence of the reduced electrical resistivity $R(T)/R(290\ \mathrm{K})$ of Ho_2Au_2In and Lu_2Au_2In.

the Pauli paramagnetism determined for Y_2Au_2Sn, Lu_2Au_2Sn, and Lu_2Au_2In.

For Dy_2Au_2Sn and Ho_2Au_2In we observe distinct anomalies at the magnetic transition temperatures. The resistivity features of Dy_2Au_2Sn are qualitatively similar to that of Dy_2Pd_2In [6]. The anomalies associated with T_N in Dy_2Au_2Sn can be interpreted in terms of superzone boundary magnetic scattering [18] which results in an increase of R/R_{290} below T_N. However it is interesting to note that the above explanation cannot be applied to Ho_2Au_2In, where R/R_{290} falls rapidly below T_C and appears to be levelling below 5 K. The strong decrease of R/R_{290} for Ho_2Au_2In (Fig. 5) can be thus attributed to the decreasing spin-disorder scattering below T_C.

Acknowledgements

We thank the Degussa-Hüls AG for a generous gift of gold wire, Mrs. E. Brücher for the susceptibility measurements, and Mrs. N. Rollbühler for determination of the resistivity behaviour. This work was financially supported by the Deutsche Forschungsgemeinschaft. S. R. is indebted to the Alexander von Humboldt Foundation for a research stipend.

[1] W. Rieger, H. Nowotny, H. Benesovsky, *Monatsh. Chem.* **1964**, *95*, 1502.
[2] R. Pöttgen, *Z. Naturforsch.* **1994**, *49b*, 1309.
[3] P. Gravereau, F. Mirambet, B. Chevalier, F. Weill, L. Fournès, D. Laffargue, F. Bourée, J. Etourneau, *J. Mater. Chem.* **1994**, *4*, 1893.
[4] M. Lukachuk, R. Pöttgen, *Z. Kristallogr.* **2003**, *218*, 767.
[5] F. Hulliger, B. Z. Xue, *J. Alloys Compd.* **1994**, *215*, 267.
[6] M. Giovannini, H. Michor, E. Bauer, G. Hilscher, P. Rogl, R. Ferro, *J. Alloys Compd.* **1998**, *280*, 26.
[7] P. Fischer, T. Herrmannsdörfer, T. Bonelli, F. Fauth, L. Keller, E. Bauer, M. Giovannini, *J. Phys.: Condens. Matter* **2000**, *12*, 7089.
[8] Ya. M. Kalychak, V. I. Zaremba, V. M. Baranyak, P. Yu. Zavalii, V. A. Bruskov, L. V. Sysa, O. V. Dmytrakh, *Izv. Akad. Nauk SSSR, Neorg. Mater.* **1990**, *26*, 94.
[9] D. Kaczorowski, P. Rogl, K. Hiebl, *Phys. Rev. B* **1996**, *54*, 9891.
[10] I. R. Fisher, Z. Islam, P. C. Canfield, *J. Magn. Magn. Mater.* **1999**, *202*, 1.
[11] F. Hulliger, *J. Alloys Compd.* **1995**, *221*, L11.
[12] F. Hulliger, *J. Alloys Compd.* **1995**, *217*, 164.
[13] R. Pöttgen, *Z. Naturforsch.* **1994**, *49b*, 1525.
[14] F. Hulliger, *J. Alloys Compd.* **1996**, *232*, 160.
[15] R. Pöttgen, Th. Gulden, A. Simon, *GIT Labor-Fachzeitschrift* **1999**, *43*, 133.
[16] A. Simon, *J. Appl. Crystallogr.* **1971**, *4*, 138.
[17] K. Yvon, W. Jeitschko, E. Parthé, *J. Appl. Crystallogr.* **1977**, *10*, 73.
[18] R. J. Elliot, F. A. Wedgwood, *Proc. Phys. Soc.* **1963**, *81*, 846.